

Strength Degradation of Brittle Surfaces: Sharp Indenters

B. R. LAWN,* E. R. FULLER, and S. M. WIEDERHORN*

Institute for Materials Research, National Bureau of Standards, Washington, D.C. 20234

A theory of strength loss for brittle surfaces in contact situations, developed in a previous paper for "blunt" indenters, is extended to the case of "sharp" indenters. A prior fracture mechanics analysis of crack growth beneath ideal cone indenters serves as the basis for predetermining the prospective surface degradation of ceramic components in service. Compared to blunt indenters, sharp indenters can cause severe degradation at lower contact loads. However, at high loads, the extent of degradation becomes remarkably insensitive to details in the indenter geometry. Essential theoretical predictions are verified by bend tests on glass slabs. Effects of indenter "sharpness" and initial specimen surface flaw state are investigated systematically, along with some secondary rate effects in the contact process. The possibility of minimizing degradation via adjustment of material parameters (including hardness) or surface condition (e.g. residual stresses, frictional properties) is briefly discussed.

I. Introduction

IN A previous paper,¹ an analysis was presented of the degradation incurred by brittle surfaces under circumstances in which indenting particles could be considered "blunt." The classical Hertzian cone crack produced beneath a hard sphere was adopted as a model representation of this situation. "Real contact" situations involving irregular particles fall somewhere between this and a second limiting type of indentation configuration, namely configurations in which the particles may be viewed as "sharp" (i.e., possessing an ideally sharp point). The contact conditions, and hence the ensuing indentation fracture patterns, are somewhat different in this second case and are not as well understood as in the cone crack configuration. Nevertheless, recent fracture mechanics studies of sharp-indenter systems²⁻⁴ provide an adequate basis for predicting degradation behavior. The present study is directed toward this end and accordingly complements the earlier study.¹

Because the deformation beneath a perfectly sharp indenter cannot be completely elastic (as it can beneath a blunt indenter), some new features are expected for the degradation properties of a given brittle material, particularly in the initiation stages of indentation fracture at low loads. At the same time, once the crack system develops well beyond the contact zone it might be anticipated that the influence of indenter geometry will become less marked. Considerations along these lines are useful in any discussion of damage in real contact processes.

As before, it will be assumed that quasistatic conditions prevail throughout the indentation process. Ideally rigid cones will be taken as typifying the sharp-indenter configuration.

II. Point Indenters and Median Penny Cracks

Essential features of the crack pattern produced in a brittle surface loaded with a hard, sharp-point indenter will be examined. The solution for the linear elastic stress field in the indented specimen prior to cracking contains a singularity about the contact point and has an inverse-square fall-off with the radial distance.^{2,3} Removal of this singularity is accounted for physically by the formation of an irreversible, stress-relieving zone of deformation (plastic or viscous flow, structural densification, etc.) around the contact; the intensity of the local stresses (characterized by the mean contact pressure) at which this deformation occurs determines the *hardness* of the material. The stress concentration immediately below the indenter point nevertheless remains high, and downward-extending cracks can be nucleated at very low loads, depending on the degree of brittleness. This condition represents a major departure from the blunt-indenter

case, where preexisting surface flaws control the crack initiation process. Indeed, if the tip region of the indenter is somehow blunted or if the preexisting flaws are sufficiently large, the formation of a small cone crack may precede the development of the deformation-induced cracks; this complication is discussed in Section IV, but for the present it may be ignored.

Once the cracks have been nucleated, they extend downward on median planes in accordance with the scheme of Fig. 1. Several mutually intersecting median cracks (depending, for example, on the symmetry of the indenter or the anisotropy of the specimen) may propagate simultaneously. However, attention will be focused on a single crack system, empirical observation showing that the depth of cracking is not too sensitive to the number of cracks formed.⁴ Variation of median-crack depth with load is described for the following stages in the growth⁴:

(1) Formation of "Contained" Median Penny Crack

Whereas in reality the nucleation of median cracks involves a threshold in the loading, for the most brittle ceramic materials this threshold is insignificantly small (typically less than one newton, as is readily evident from hardness test observations). The cracks assume the form of well-defined pennies, wholly contained below the contact zone, and grow downward stably as the load is applied. This configuration constitutes a complex elastic-plastic problem. A simplified fracture mechanics analysis² indicates that, in addition to the usual fracture parameters, namely the fracture surface energy Γ and the Young's modulus E , the hardness H should enter into the relation between indenter load and crack size; the scale of the deformation zone determines the degree of stress relief that occurs about the singular point in the ideally elastic field. A second analysis, based on a more or less dimensional argument for general penny-shaped cracks, predicts a slightly different relation between the parameters.⁴ Although less explicit in the dependence on hardness, the second treatment provides a better empirical fit to crack growth data and will therefore be cited here.

Presented at the 77th Annual Meeting, The American Ceramic Society, Washington, D.C., May 6, 1975 (Basic Science Division, No. 42-B-75). Received May 27, 1975; revised copy received October 31, 1975.

Sponsored by the Office of Naval Research under Contract No. NR-032-535.

*Member, the American Ceramic Society.

*On study leave from School of Physics, University of New South Wales, Kensington, N.S.W. 2033, Australia.

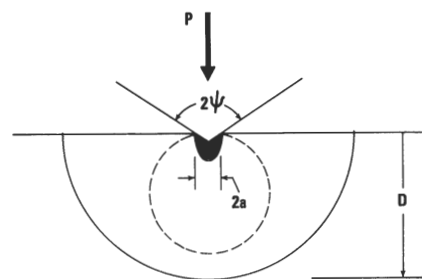


Fig. 1. Median crack parameters. Crack nucleates at extremity of deformation zone below indenter point and forms into a penny wholly contained beneath contact surface (broken circle). At some critical load the crack breaks through spontaneously to the free surface ("pop-in"), usually with attendant increase in crack depth, D , and transforms into a well-developed half-penny configuration (solid semicircle). This transformation may also be effected in an alternative stable manner, via the action of residual stresses about the deformation zone on unloading of the indenter prior to pop-in.

Accordingly, for smooth indenters,

$$P^2/D^3 = 2\Gamma E/\kappa_D^f(\nu, H/E, \psi) \quad (1)$$

where P is the load on the indenter, D is the depth of the crack (the penny diameter for the contained median penny crack), ν is Poisson's ratio, ψ is the cone half-angle, and κ_D^f is a dimensionless factor (f signifying *formation* stage of crack growth) whose value needs to be determined by experimental calibration. It may be noted that this equation does not involve the state of the specimen surface (flaw population, etc.). However, the angle of the cone, through its influence on the indentation field, does enter as a variable.

Up to this point the cracks cannot be considered to be "well-developed," for they still remain within the sphere of influence of the nucleation zone immediately below the contact. However, there is a critical configuration, albeit ill-defined, above which the contact zone can no longer contain the expanding penny ($D \gg a$, Fig. 1).^{*} At this point the crack "breaks through" to the specimen surface, and thereby becomes fully propagating.

(2) Propagation of "Center-Loaded" Median Half-Penny Crack

Beyond the breakthrough load the median crack assumes the form of a center-loaded half-penny crack (radius D , Fig. 1). Details of events at the contact zone no longer exert a strong influence on the fracture mechanics: the crack has escaped the nucleation forces and is now controlled by the component of the applied load which acts to wedge open the mouth region. Nevertheless, the crack geometry retains the essential features of a (somewhat modified) penny configuration, in which case for smooth indenters the analogy to Eq. (1) is the relation

$$P^2/D^3 = 2\Gamma E/\kappa_D^p(\nu, \psi) \quad (2)$$

with κ_D^p another dimensionless factor (p signifying *propagation* stage of crack growth); we note that the hardness now disappears from the fracture mechanics calculation. A straightforward analysis, based on a center-loaded, full penny in an infinite solid, gives⁴

$$\kappa_D^p(\nu, \psi) = (1 - \nu^2)/\pi^3 \tan^2 \psi \quad (3)$$

Generally, the contact will not be smooth. It can be shown that the effect of including frictional tractions at the indenter-specimen interface is simply to replace ψ by $\psi' = \psi + \arctan \mu$ (μ = coefficient of friction), i.e., effectively to "blunt" the indenter tip.⁴ The effect of ignoring friction is therefore to overestimate κ_D^p in Eq. (3), and hence D in Eq. (2). In other words, we deal with a "worst case" situation.

In practice, the transition from stage (1) to stage (2) in the growth of a given median crack can be detected, either by direct observation of the indentation process (in transparent solids), by monitoring the acoustic emissions as the contained penny pops through to the specimen surface, or by recording load drops in a fixed-grips loading arrangement. While such discontinuities in growth occur at generally lower critical loads as the cone half-angle diminishes, the critical loads themselves vary considerably under apparently constant indentation conditions. Moreover, mutually intersecting median cracks may "pop-in" at different stages in the loading and accordingly be retarded in further growth by their less-developed neighbors. Multiple-cracking complications are particularly noticeable at the lower cone angles. This aspect of the indentation cracking remains poorly understood.

(3) Residual Median Crack

Unlike the elastic-brittle contact of the ideally blunt indenter situation,¹ the present case is complicated by further developments in the crack pattern upon *unloading*. Incompatibility between the stress-strain responses of nonlinear material within the irreversible deformation zone and linear material without gives rise to mismatch tractions at the contracting zone boundary. The net result is a residual stress field which begins to dominate the field of the applied loading just prior to complete removal of the indenter. This residual field contains a component of tension sufficiently intense to generate an entirely new, laterally extending system of cracks.^{2,5} How-

ever, such lateral cracks are relatively shallow, and thus do not contribute significantly to degradation. A more important influence of the residual stresses here is evident in the behavior of contained penny cracks already formed during the preceding, *loading* half-cycle. These cracks progressively grow toward the specimen surface as the indenter is withdrawn; an alternative route to the fully developed form thereby exists, without the need for the critical pop-in load ever to be exceeded.⁴

Thus the final state of the strength-controlling median crack system inevitably approaches the half-penny configuration, regardless of the loading history. This configuration is most commonly evidenced by the appearance of characteristic radial traces of the median cracks on the indented surfaces. The dimensions of these traces tend to reflect the depth of cracking one would anticipate if the half-penny configuration were to be realized *prior* to maximum loading.⁴ With this information Eq. (3) may be used for fully developed median cracks to determine the effect of indenter "sharpness" (all else being constant) on the resultant crack size. Figure 2 is an appropriate plot of $[\kappa_D^p(\psi)]_v$ for cone indenters on glass, with $\nu = 0.25$. Experimental data from indentation observations, for tungsten carbide indenters on glass surfaces in air environments, fall somewhat below the calculated curve, suggesting that the effects of friction are not insignificant here. Nevertheless, we shall proceed for the present on the basis of a smooth contact, mindful that the resulting upper limit $\kappa_D^p(\psi)$ to be used in Eq. (2) will lead to an overestimate in D , thus providing a conservative value for the strength of the indented surface.

III. Strength Degradation Tests

(1) Test Procedure

The standard Griffith formula for the rupture stress σ in a homogeneous tensile field again provides the basis for the strength tests:

$$\sigma = [2\Gamma E/\pi(1 - \nu^2)c_f]^{1/2} \quad (4)$$

where c_f is the effective flaw size of an equivalent through crack. Of the variables in Eq. (4), it is the flaw size which is most susceptible to extraneous influences (mechanical, thermal, chemical, etc.).

Soda-lime silicate glass laths for four-point bend testing were prepared as in the previous study,¹ with one or two minor differences. In the present case, the 10 μm level of preexisting flaws typical of carefully handled ceramic surfaces is eclipsed by the extent of median cracking produced at indentation loads as low as 1 N. As-received laths hence provided perfectly adequate test surfaces for the bulk of the testing, although the test areas of one set of

^{*}This condition in turn implies a critical load, since, taken together with the definition of hardness, $H = P/\alpha\pi a^2$ (α = a geometrical factor, which is unity for cone indenters), Eq. (1) predicts, for a fixed value of H , $D/\alpha \propto P^{1/6}$.

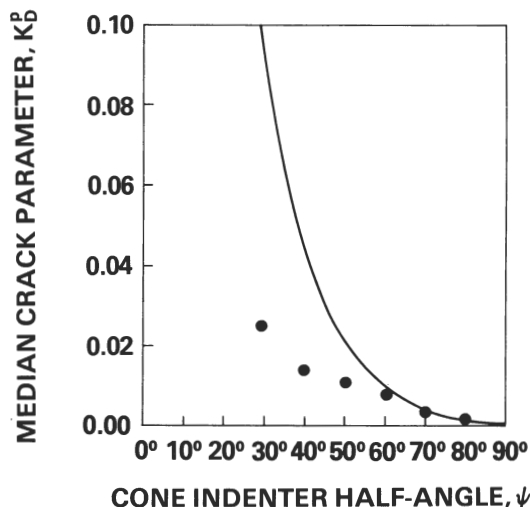


Fig. 2. Plot of $\kappa_D^p(\psi)$ from Eq. (3) (solid line) for glass. Data points (circles) represent measurements made in air using WC indenters (Ref. 4).

specimens were preabraded by a grit-blast treatment¹ to determine whether severe preexisting surface damage produces any side effects in the indentation process.

For each specimen the prospective indentation site was covered with a drop of paraffin oil to prevent moisture-assisted slow crack growth during subsequent testing. (In the case of grit-blasted specimens, the abraded area was covered immediately after the treatment.) Each specimen surface was then indented with a tungsten carbide conical indenter of given half-angle ψ , at a prescribed load P . (The tip radius of the cones used never exceeded $5\text{ }\mu\text{m}$ throughout the experiments.) The specimens were then loaded to rupture with the indented surface in tension. Unless specified otherwise, the bend test was effected within 4 h of indenting in the experiments reported here.

Examination of the laths after breaking indicated that the indentation site was the origin of fracture in the vast majority of tests. Isolated edge failures did occur, and these were rejected from the data accumulation. Reproducibility in strength values was limited mainly by variations in the indentation crack pattern under any specified set of test conditions; the scatter in data points in the figures to follow therefore indicates the experimental accuracy.

(2) Strength of Indented Test Pieces

Strength degradation was investigated as a function of indentation load for different cone half-angles. Up to a (very low) limiting load, e.g. P' , the rupture stress maintained the level characteristic of the unindented surface (depending on the prior history of the glass specimens). In this region of behavior the effective length of the dominant flaw is presumably determined by the size of preexisting microcracks, i.e., $c_f = c_f^0$ when $(P \leq P')$. Above the limiting load the rupture stress declined steadily. The effective flaw length here becomes a function of the size of median cracks, i.e., $c_f = c_f(D)$, ($P > P'$): an analysis of penny cracks in a tensile field gives the explicit relation $c_f \approx (4/\pi^2)D$. With Eq. (2), this result makes it possible to rewrite the strength equation, Eq. (4), in terms of indentation load, for a given cone, under fixed test conditions,

$$\sigma = [2\Gamma E / \pi(1 - \nu^2)c_f^0]^{1/2} \quad (P \leq P') \quad (5a)$$

$$\sigma = \{(2\Gamma E)^{2/3} \pi^{1/2} / 2(1 - \nu^2)^{1/2} [\kappa_D^p(\nu, \psi)]^{1/6}\} P^{-1/3} \quad (P > P') \quad (5b)$$

These equations may be evaluated in terms of readily measurable fracture mechanics parameters. For WC cone indenters on soda-lime glass the values are: $E = 7.0 \times 10^{10}\text{ Nm}^{-2}$, $\nu = 0.25$, and $\Gamma = 3.9\text{ Jm}^{-2}$ (glass data⁶); κ_D^p : $(30^\circ) = 9.0 \times 10^{-2}$, $(40^\circ) = 4.3 \times 10^{-2}$, $(50^\circ) = 2.0 \times 10^{-2}$, $(60^\circ) = 1.1 \times 10^{-2}$, $(70^\circ) = 5.0 \times 10^{-3}$, and $(80^\circ) = 1.5 \times 10^{-3}$ (as per the curve in Fig. 2), leaving c_f^0 and ψ as test variables; the second has the more interesting implications.

(A) *Effect of Flaw Size*: A preliminary indentation/strength test was conducted to check the effect of initial surface state on degradation. In Fig. 3 results are compared for surfaces as-received and grit-blasted (No. 100 SiC grit, corresponding to $c_f^0 = (23 \pm 5)\text{ }\mu\text{m}$),¹ for a cone of half-angle 70° . Also included in the figure are the theoretical predictions (full lines) of Eqs. (5a) and (5b). Other than at low loads, where the abrasion flaws dominate the indentation damage in the case of grit-blasted surfaces, the results are indistinguishable. Consequently, for the remainder of the tests it suffices to work simply with as-received surfaces.

(B) *Effect of Cone Angle*: The most extensive tests were directed to an investigation of the role of indenter sharpness in surface degradation. Figure 4 illustrates the experimental data and the theoretical curves from Eq. (5). Agreement here is reasonable, taking into account the spread in the data, although some discrepancy is apparent at the largest cone angle, $\psi = 80^\circ$. Note that the strength behavior is not highly sensitive to indenter sharpness, except perhaps again at the larger angles, notably at $\psi = 80^\circ$. Also the strength fall-off is remarkably slight with increasing indenter load. That the loads attained in these experiments are substantial is borne out by the fact that the sharper cones quickly became rounded (in which case their tips were reground), and the glass beneath the contact began to crush at levels not much higher than those represented in Fig. 4.

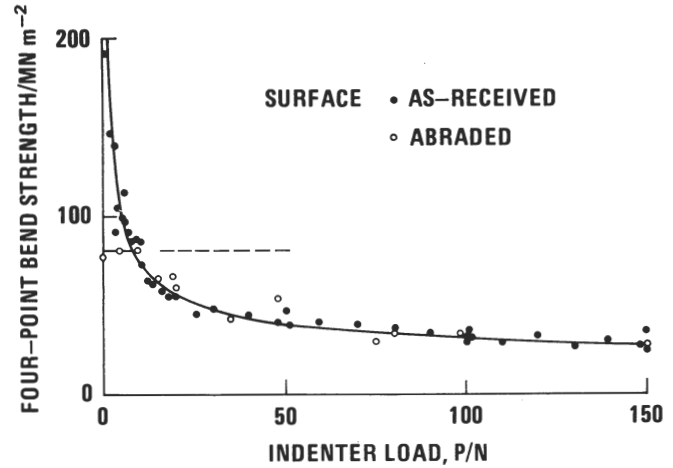


Fig. 3. Strength of soda-lime glass surfaces (as-received and abraded with No. 100 SiC grit) as function of indentation load for given WC cone, $\psi = 70^\circ$. Theoretical predictions (solid lines) from Eq. (5). Oil environment; crosshead speed 0.5 mm min^{-1} for indentation tests and 50 mm min^{-1} for bend tests.

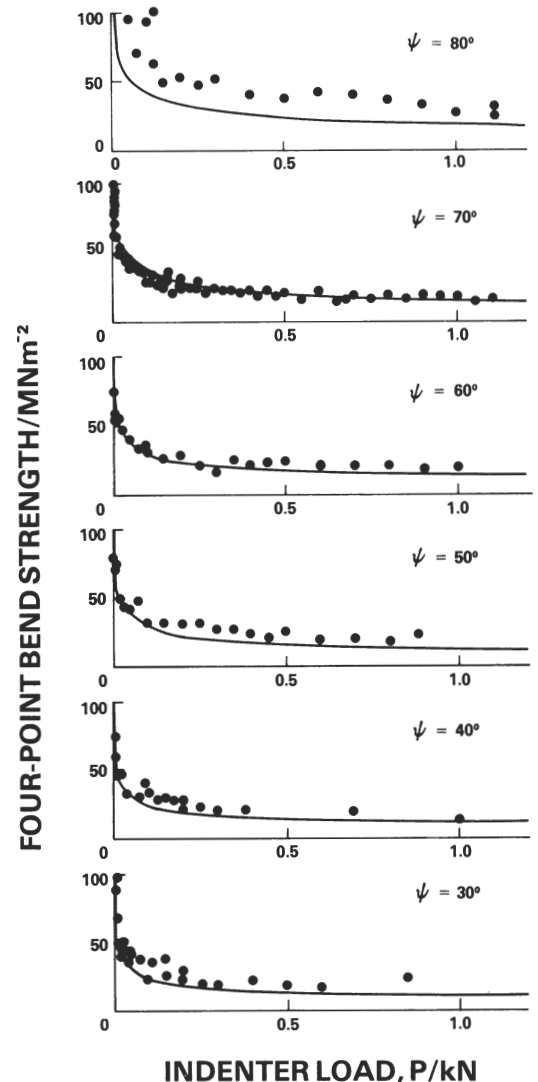


Fig. 4. Strength of as-received soda-lime glass surfaces as function of indentation load for WC cones with half-angles indicated. Theoretical predictions (solid lines) from Eq. (5). Oil environment; crosshead speed 0.5 mm min^{-1} for indentation tests and 50 mm min^{-1} for bend tests.

(C) *Some Secondary Rate Effects:* Finally, two interesting time-dependent effects observed by Holland and Turner,⁷ in analogous strength-loss tests on scratched glass surfaces, were briefly examined. In the first, Holland and Turner noted a tendency for specimens to slowly recover their strength as the delay between indentation and rupture in bending was prolonged. Figure 5 confirms this effect, for the specific case of normal indentation at $\psi = 70^\circ$, $P = 100$ N. However, the recovery is significant only for aging times of 1 day or more and therefore is not a factor in the results reported earlier in this study.

In the second effect, which relates to load-rate effects, Holland and Turner reported a drop of $\approx 20\%$ in strength values as the scratch velocity was increased over a range 0 to 5 ms^{-1} , at normal load $P = 5$ N. Results of a parallel experiment, in which the crosshead speed to a peak (quasistatic) normal indentation load $P = 100$ N was varied over four orders of magnitude, are shown in Fig. 6. There is no evidence of a rate effect.

IV. Discussion

The present model establishes a basis for predicting *a priori* the prospective strength degradation in contact situations where the indenting particles can be considered "sharp." Comparing the strength equation, Eq. (5), with its counterpart for blunt indenters in the earlier study,¹ shows again that degradation is minimized for surfaces of large characteristic Γ (tough), E (stiff), and ν (tension-inhibiting, in basically compressive loading). Further, we might anticipate, following the description of Section II (1), that low values of H would be of advantage in suppressing the formation of indentation-induced cracks at low loads; the role of hardness will be discussed again later.

A major distinction between the cases of sharp and blunt indenters arises in connection with the state of the brittle surface prior to indentation. Whereas with blunt indenters preexisting surface flaws exert an important influence through control of fracture initiation processes, the same is not true with sharp indenters, which induce their own flaws. On the other hand, there are other aspects of the surface condition which may have significant effects in crack initiation *independently* of indenter geometry. An example is the fracture-inhibiting effect of residual compressive stresses in a toughened surface. All such effects will be manifest at lower indentation loads, where the indentation cracks remain within the sphere of influence of the near-contact region. Generally, however, the more pointed indenters, by virtue of their greater capacity to concentrate stresses, produce the most severe damage in this domain.

At higher loads the differences due to details in the near-contact conditions tend to "wash out." In their well-developed form, all indentation cracks inevitably assume some modified penny configuration,⁴ the growth of which becomes determined by the stresses of "point loading." The field in this limit is radial (inverse-square fall-off) about the contact point, which explains the parallel behavior, toward the upper end of the indentation load scale, between the strength-loss curves in Fig. 4 of the present paper and Figs. 3 and 4 of Ref. 1. There is accordingly less need to take into account

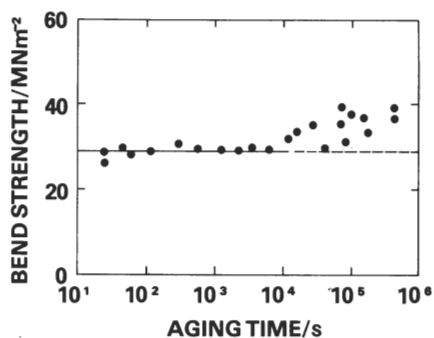


Fig. 5. Strength of as-received soda-lime glass surfaces as function of time of aging between indentation and bend testing. Data for WC cone $\psi = 70^\circ$, $P = 100$ N, oil environment; crosshead speed 0.5 mm min^{-1} for indentation and 50 mm min^{-1} for bending.

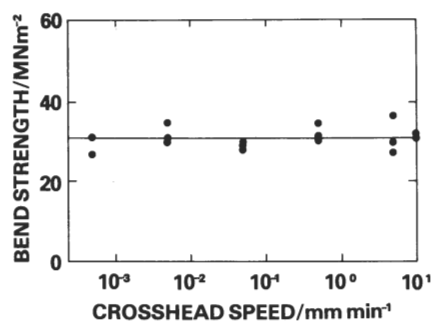


Fig. 6. Strength of as-received soda-lime glass surfaces as function of crosshead speed in indentation test. Data for WC cone $\psi = 70^\circ$, $P = 100$ N, oil environment; crosshead speed for bend tests 50 mm min^{-1} .

specifics of indenter geometry when the contact damage is severe. Moreover, while sharper indenters do tend to produce deeper cracks at a given load,⁴ these same indenters tend also to become flattened at the tip or to severely crush the supporting surface. Further, to produce these deeper cracks the sharper indenter must penetrate further between the crack walls, i.e., it must do more work. The implication here is that in situations in which the indentation event is governed by a fixed energy input (e.g. in a fixed-velocity impact situation) the effects of indenter sharpness may well disappear altogether.⁸

Nevertheless, taking a broad view of the strength degradation curves obtained in this and the earlier study, the degree of indenter sharpness, as signified by the cone half-angle (or sphere radius), remains an important factor to be considered, particularly in relation to the interpretation of degradation processes in "real contact situations." Here it may be feasible to characterize a sharp indenting particle by some "effective half-angle" (note, for instance, that a Vickers pyramid, whose opposing faces subtend an angle of 136° , produces cracks in glass of very much the same depth as does a cone of $\psi = 70^\circ$). However, in most cases the assignment of a simple index of sharpness will not be so straightforward. Even the sharpest particles must in reality have a finite nonzero tip radius, so the possibility exists of a gradual "blunt-sharp transition" in the strength response with increasing severity of indentation.* An opposite, "sharp-blunt transition," corresponding to an increasing argument in the tangent term of Eq. (3), may be realized in cases where frictional effects become pronounced.† The most general real contact situation is clearly very complex indeed.

Friction is a further factor which warrants a good deal more attention than has been possible in the present study. It should be emphasized that the present tests were conducted under oil. In a different environment the frictional properties of the indenter/specimen contact interface could be quite different. In most instances it would be wise to base any strength design criterion on the conservative assumption that frictional tractions are entirely absent (thereby overestimating the depth of indentation cracking). On the other hand, the possibility is raised of fabricating surfaces in such a way that the operative frictional forces are deliberately made large, in order to suppress the relatively dangerous median fracture system.

Finally, a number of secondary effects are associated with nonequilibrium, and history-dependent, crack configurations. Several of these effects have been discussed in the earlier work¹; only

*The corresponding change in fracture pattern in such a case has been well demonstrated by K. Phillips, whose results are illustrated in Fig. 21 of Ref. 3.

†As mentioned in Section II (2), the effective cone angle ψ' when friction is present is $\psi + \arctan \mu$. Thus, for the indentations corresponding to $\psi = 80^\circ$ in the present experiments, a friction coefficient $\mu \approx 0.2$ gives $\psi' \approx 90^\circ$, a "perfectly blunt" indenter. In this one case, examination of the cone-indented specimens revealed that Hertzian cone fracture, typical of ideally blunt indenters, forms at the expense of the median fracture system (Ref. 4). The data points in the plot for $\psi = 80^\circ$ in Fig. 4 do, in fact, fit reasonably well to the degradation curve predicted for well-developed cone cracks (Ref. 1). In this description, the cone-crack curve provides an upper limit to the strength resulting from any sharp-point contact situation.

one new aspect is briefly considered here. We have already indicated the possible role of the irreversible deformation properties of the indented solid, as characterized by the hardness, in controlling the initial stages of crack growth. The hardness of glasses⁹ and many other brittle materials¹⁰ is strongly rate-dependent, so additional kinetic effects in the strength degradation curves might be expected, particularly at lower loads where the inelastic processes appear to have some influence on the crack formation (Sections II (1), II (3)). The null effect observed in Fig. 6 may arise from the fact that our tests were conducted under oil, an environment which tends to minimize the time dependence of the hardness of glass.⁹ The analogous experiments by Holland and Turner (Section III), on the other hand, were conducted in an ordinary laboratory atmosphere: their positive effect, in which the strength was observed to diminish with velocity of the scratch indenter, correlates with a corresponding increase in hardness of glass with decreasing contact duration in air.⁹ This aspect is interesting and invites further, special attention, particularly in connection with less brittle ceramic materials.

Acknowledgments: The writers are grateful to A. G. Evans for stimulating discussions relating to this work.

References

- ¹ B. R. Lawn, S. M. Wiederhorn, and H. H. Johnson, "Strength Degradation of Brittle Surfaces: Blunt Indenters," *J. Am. Ceram. Soc.*, **58** [9-10] 428-32 (1975).
- ² B. R. Lawn and M. V. Swain, "Microfracture Beneath Point Indentations in Brittle Solids," *J. Mater. Sci.*, **10** [1] 113-22 (1975).
- ³ B. R. Lawn and T. R. Wilshaw, "Indentation Fracture: Principles and Applications," *ibid.*, [6] 1049-81.
- ⁴ B. R. Lawn and E. R. Fuller, "Equilibrium Penny-Like Cracks in Indentation Fracture," *ibid.*, **10** [12] 2016-24.
- ⁵ B. R. Lawn, M. V. Swain, and K. Phillips, "On the Mode of Chipping Fracture in Brittle Solids," *ibid.*, [7] 1236-39.
- ⁶ S. M. Wiederhorn, "Fracture Surface Energy of Glass," *J. Am. Ceram. Soc.*, **52** [2] 99-105 (1969).
- ⁷ A. J. Holland and W. E. S. Turner, "Effect of Transverse Scratches on the Strength of Sheet Glass," *J. Soc. Glass Technol.*, **21** [87] 383-94T (1937).
- ⁸ S. M. Wiederhorn and Brian Lawn; unpublished work.
- ⁹ S. P. Gunasekera and D. G. Holloway, "Effect of Loading Time and Environment on the Indentation Hardness of Glass," *Phys. Chem. Glasses*, **14** [2] 45-52 (1973).
- ¹⁰ R. E. Hanneman and J. H. Westbrook, "Effects of Adsorption on the Indentation Deformation of Non-Metallic Solids," *Philos. Mag.*, **18** [151] 73-88 (1968).